Culture of equine fibroblast-like synoviocytes on synthetic tissue scaffolds towards meniscal tissue engineering: a preliminary cell- seeding study

1) Jennifer J. Warnock, Comparative Orthopaedic Laboratory, University of Missouri, Columbia, MO; Dr. Warnock's current address is College of Veterinary Medicine, Oregon State University, Corvallis OR

2) Derek B. Fox, Comparative Orthopaedic Laboratory, University of Missouri, Columbia, MO;

3) Aaron M. Stoker, Comparative Orthopaedic Laboratory, University of Missouri, Columbia, MO

4) Mark Beatty, VA Nebraska-Western Iowa Health Care System and University of Nebraska Medical Center College of Dentistry, Lincoln, NE

5) Mary Cockrell, Comparative Orthopaedic Laboratory, University of Missouri, Columbia, MO

6) John C. Janicek, Comparative Orthopaedic Laboratory, University of Missouri, Columbia, MO; Dr. Janicek's current address is Brazos Valley Equine Hospital Navasota, TX 77868

7) James L. Cook, Comparative Orthopaedic Laboratory, University of Missouri, Columbia, MO

,

CORRESPONDING AUTHOR:
Jennifer J. Warnock,
Dr. Warnock's current address is:
Magruder Hall, College of Veterinary Medicine
Oregon State University, Corvallis OR 97331
541-737-4812
jennifer.warnock@oregonstate.edu

Introduction:

The knee menisci are semilunar-shaped fibrocartilages with extracellular matrix (ECM) composed primarily of types I and II collagen, glycosaminoglycans (GAGs), and water (Fithian et al. 1990). It is now well established that intact menisci are crucial for the maintenance of normal joint function, however these critical structures are frequently injured in humans and animals. Meniscal tears are the most common knee injury in people, and arthroscopic meniscectomy represents the most common human orthopedic surgery performed annually (Burks et al. 1997). Meniscal injuries are also a significant cause of lameness and decreased performance in horses (Peroni & Stick 2002; Walmsley 1995; Walmsley et al. 2003); equines affected by naturally occurring meniscal tears may also be a viable model for the study of human meniscal injury.

As the axial, avascular portion of the meniscus has a limited ability to heal spontaneously, (Arnoczky & Warren 1983; Kobayashi et al. 2004), the majority of meniscal injuries are treated with partial menisectomy. However, this also results in eventual articular cartilage damage of the tibia and femoral condyles, and progression of debilitating osteoarthritis (Arnoczky & Warren 1983; Cox et al. 1975). Thus tissue engineering new meniscal fibrocartilage is being investigated as a treatment for avascular meniscal injuries.

Synovium may be an ideal cell source for meniscal tissue engineering. Synovium plays an important role in attempted vascular zone healing and regeneration (Cisa et al. 1995; Kobuna et al. 1995; Ochi et al. 1996; Shirakura et al. 1997). Synovium has the ability to form fibrocartilaginous-like tissue *in vivo* in response to meniscectomy (Cox et al. 1975). In addition, synoviocytes have been reported to be an important element in cellular repopulation of meniscal allografts (Arnoczky & Warren 1983; Rodeo et al. 2000). Synovial tissue progenitor cells,

56   grossly indistinguishable in culture from type B or fibroblast-like synoviocytes (FLS), can

57   undergo chondrogenesis *in vitro* (De Bari et al. 2001; Nishimura et al. 1999). Taken together,

58   these data indicate that synovium may be able to serve as a source for functional fibrocartilage

59   in engineering meniscal tissue, provided the chondrogenic potential of synoviocytes can be

60   optimized.

61   Tissue engineering scaffolds must provide substrate and stability for cellular retention,

62   intercellular communication, and cellular growth to allow seeded cells to proliferate extracellular

63   matrix (ECM). As the scaffolds naturally degrade, the cellular ECM must be able to take on the

64   biomechanical function and form previously designated by the scaffolds to maintain construct

65   integrity. Thus a scaffold must be hydrophilic enough to allow cell adhesion but have a long

66   enough half- life to not prematurely dissolve, which would prevent ECM proliferation and cell

67   death. PGA (poly -glycolic acid) and PLA (poly-L- lactic acid) are biodegradable,

68   biocompatible, poly-esters, that are attractive for tissue engineering because they are readily

69   available, can be easily processed into a variety of structures, and are approved by the Food and

70   Drug Administration for a number of biomedical applications (Lavik et al. 2002). PGA has been

71   successfully used as a scaffold for meniscal fibrochondrocytes *in vivo* (Kang et al. 2006) and

72   cultured *in vitro* (Aufderheide & Athanasiou 2005) to form meniscal-like tissue. Another

73   scaffold type, PLLA, (poly-L lactic acid) has been successfully used for *in vitro* tissue

74   engineering of leporine meniscal fibrochondrocytes (Esposito et al. 2013; Gunja & Athanasiou

75   2010), chondrocytes (Sherwood et al. 2002), and human fibroblasts (Hee et al. 2006). PGA –

76   PLLA combinations have also been successfully used for *in vitro* meniscal culture (Ionescu &

77   Mauck 2013). In addition, chondrocytes cultured on PGA-PLLA mixtures versus collagen sheets

78   contain more collagen type II and have stronger mechanical properties (Beatty et al. 2002) than

79   single polymer scaffolds. Further investigation of combination use of PLLA combined with

80   PGA for *in vitro* synoviocyte culture is warranted.

81   Cartilage and fibrocartilage engineering with biodegradable scaffolds is most successful

82   if uniform cell distribution is achieved (Davisson et al. 1999; Pazzano et al. 2000; Smith et al.

83   1995), which is optimized through the use of rotating bioreactors(Aufderheide & Athanasiou

84   2005; Kim et al. 1998; Pazzano et al. 2000). In addition, rotating bioreactors provide mechanical

85   stimulation of cultured cells. This has a positive effects on cell differentiation, cell viability,

86   extracellular matrix production, and compressive biomechanical properties, through

87   mechanotransductive effects (Davisson et al. 1999; Imler et al. 2004; Pazzano et al. 2000; Smith

88   et al. 1995). Thus scaffold culture in a rotating bioreactor may represent a useful technique for

89   synoviocyte- based engineering of functional meniscal tissue.

90   Based on this prior research, we believe that both PGA and PLLA would be viable

91   synthetic scaffolds for the *in vitro* culture of FLS for application in meniscal fibrocartilage tissue

92   engineering. Thus, the first objective of this study was to 1) determine cell distribution and ECM

93   formation of equine FLS seeded and cultured dynamically in a rotating bioreactor versus static

94   seeding and culture, on two synthetic scaffold types, PGA and open- cell PLLA (OPLA). The

95   second objective was to compare cell viability, distribution, and ECM formation of FLS cultured

96   on 2% vs 4% PLLA coated PGA scaffolds, cultured for 14 or 21 days. Our hypothesis was that

97   we would see no difference in equine FLS content, FLS distribution, and ECM formation

98   between scaffold type, biomechanical culture environment, and culture duration.

99   **Materials and Methods:**

100   ***Experiment 1:***

101   *Tissue Collection and Monolayer Cell Culture*-- Six 8.0 mm x 8.0 mm biopsies of

102   synovial intima and subintima were obtained from both stifles of an adult American Quarter

103   Horse, euthanatized according the American Veterinary Medical Association's guidelines for

104   humane euthanasia, for reasons unrelated to the study. The horse was determined to be free of

105   orthopedic disease based on pre-mortem physical examination and post mortem gross

106   examination of the joint. Tissue was placed in Dulbeccos' Modified Eagle's Media (DMEM)

107   with 10% fetal bovine serum, 0.008% Hepe's buffer, 0.008% non-essential amino acids, 0.002%

108   penicillin 100I.U./mL streptomycin 100ug/mL, amphoterocin B 25ug/mL, 0.002% L-ascorbate,

109   and 0.01% L-glutamine in preparation for monolayer culture.

110   Synovium was sectioned into 2.0mm x 2.0mm pieces using a #10 Bard Parker blade

111   under sterile conditions. The tissue fragments were combined with sterile Type 1A clostridial

112   collagenase solution (Type 1A Clostridial Collagenase, Sigma, St. Louis, MO) at a concentration

113   of 7.5mg/mL of RPMI 1640 solution. The mixture was agitated at 37°C, 5% CO_2, 95%

114   humidity for six hours. Cells were recovered through centrifugation, the supernatant decanted

115   and the cellular pellet re-suspended in 5mL of supplemented DMEM. The cell solution was

116   transferred to a 25cm^2 tissue culture flask containing 5mL of supplemented DMEM. The flasks

117   were incubated at 37°C, 5% CO_2, 95% humidity, with sterile medium change performed every 3

118   days. Synovial cells were monitored for growth using an inverted microscope until observance

119   of 95% cellular confluence per tissue culture flask. At second passage cells were transferred to

120   75cm^2 tissue culture flasks containing 11mL of media. At 95% confluence the cells were

121   subcultured until the 4th cell passage had been reached. At 4th passage cells were removed from

122   flasks, counted using the Trypan Blue exclusion assay (Strober 2001), and transferred to scaffold

123   culture as described below.

124   *Scaffolds*—A non- woven polyglycolic acid (PGA, Tissue Scaffold, Synthecon, Houston,

125   TX) felt, 3mm thick, with 10μm diameter fibers was utilized for this study. The open-cell poly-

126   lactic acid (OPLA sponge, BD Biosciences, Bedford, MA) utilized were 5.0mmx 3.0mm, non

127   compressible, cylindrical sponges. The average OPLA sponge pore size was 100-200μm with a

128   hydration capacity of 30μl/ scaffold. PGA and OPLA scaffolds were sterilized in ethylene oxide.

129   Following sterilization, the PGA felt was cut using a sterile Baker's biopsy punch to create into

130   5.0mm x 3.0mm discs prior to cell culture to match the dimensions of the OPLA scaffolds.

131   *Dynamic Culture*-- Twelve PGA scaffolds (PGA-D group) and 12 OPLA sponges

132   (OPLA- D group) were placed in separate 110mL vessel flasks of a rotating bioreactor system

133   (Rotating Bioreactor System, Synthecon, Houston, TX (Fig. 1) containing 110mL of

134   supplemented DMEM. The scaffolds were presoaked for 24 hours in the bioreactor at 37˚C, 5%

135   CO2, 95% humidity, prior to cell introduction. Fourth passage FLS were removed from the

136   tissue culture flasks enzymatically (Accutase Innovative Cell Technologies, San Diego, CA) and

137   counted. Cells were added to the 110mL bioreactor flasks at a concentration of 1 million cells/

138   scaffold via a 60cc syringe, slowly injected over several minutes. For the duration of the study

139   the bioreactor vessels were rotated at 51.1 rpm to allow the scaffolds to free-float and rotate

140   within the culture medium, without contacting the inner bioreactor surfaces. Cultures were

141   maintained at 37˚C, 5% CO2, 95% humidity. Fifty percent of the cell culture medium volume

142   was changed using sterile technique every 3 days. Cell counts were performed on discarded

143   media for the first two media changes.

144   *Static Culture*-- Twelve PGA scaffolds (PGA-S group) and 12 OPLA sponges (OPLA-S

145   group) were placed individually in non- treated 24 well tissue culture plates, each well

146   containing 2mL of supplemented DMEM (Fig. 2). The scaffolds were presoaked for 24 hours at

147 37˚C, 5% CO2, 95% humidity, prior to cell introduction. Then FLS were transferred from

148 monolayer culture as described above, and slowly over 3 minutes, pipetted on top of the

149 scaffolds in solution, at 1 million cells per scaffold in each well. The plates were maintained at

150 37˚C, 5% CO2, 95% humidity, with 50% cell culture medium changed every 3 days. Cell counts

151 were performed on discarded media for the first 2 media changes.

152   *Histologic Analysis*-- All scaffolds were harvested on the 12th day of culture. Six

153 scaffolds from each group (PGA-S, PGA-D, OPLA-S, OPLA-D) were fixed in 10% buffered

154 formalin, embedded in paraffin, sectioned, and stained with Masson's Trichrome, Safranin –O,

155 and Hematoxylin and Eosin. Histologic specimens were examined at 10x magnification (Zeiss

156 Microscope, Carl Zeiss, Thornwood, NY). Images of each section, (three from the scaffold

157 periphery and three from the scaffold center) at 2 o'clock, 6o'clock and 10o'clock positions (Fig.

158 3) were digitally captured by a digital camera (Olympus DP-70 Olympus, Melville, NY) and

159 saved as tagged- image file format images. Digital image analysis was performed as previously

160 validated (Amin et al. 2000; Benzinou et al. 2005; Girman et al. 2003; Goedkoop et al. 2005)

161 whereby cellular density was assessed using a thresholding algorithm (Loukas et al. 2003) using

162 computer image analysis (Fovea 3.0, Reindeer Graphics, Asheville, NC). This algorithm allows

163 quantification of cellular nuclei based on their histogram values. All cell counts were

164 additionally validated by hand counts. Safranin-O staining, indicating presence of GAG, and

165 Masson's Trichrome staining, indicating presence of collagen, were subjectively evaluated and

166 recorded.

167   *Biochemical ECM Analysis*-- Three cultured scaffolds from each group were analyzed for

168 glycosaminoglycan (GAG) and collagen production. Wet weight of each scaffold was obtained.

169 GAG content of the scaffold was performed using the Dimethylmethylene Blue Sulfated

170   Glycosaminoglycan assay (Farndale et al. 1986). Collagen content of the cultured scaffolds was

171   assessed using the hydroxyproline assay, as described by Reddy et al.(Reddy & Enwemeka

172   1996).

173   *Statistical Methods*—Data were tested for normality using a Shapiro-Wilk test.

174   Data were then analyzed using a one way analysis of variance followed by a Tukey's test, to

175   compare the effect of scaffold type and seeding technique on cell counts and ECM quantity. To

176   determine significance between periphery and central cell counts within each scaffold, a paired,

177   2-tailed student's t-test was performed. For all tests significance was set at P <0.05.   All

178   statistical analyses were performed using a statistical software program, (GraphPad Prism

179   Version 6, San Diego, CA).

180   .

181   *Experiment 2:*

182   *Scaffolds*-- Poly-L –Lactic acid (PLLA) was dissolved in methylene chloride as a 2% or

183   4% solution. The 2% and 4% PLLA solution each was applied to a 3.0 mm thick sheet of the

184   same, above- described, non- woven PGA felt, using an eye-dropper. Following PLLA

185   treatment, the treated felt was placed in a vacuum dessicator overnight and then sterilized in

186   ethylene oxide. Following sterilization, the 2% and 4% PLLA modified PGA felts were cut into

187   fourteen 5mmx 7mmx 3mm square scaffolds using sterile scissors and a #10 bard parker blade

188   (Fig 4).

189   *Tissue Collection and Monolayer Cell Culture* -- Synovial intima/ subintima was

190   harvested from the stifles of two mixed breed, adult horses euthanatized according the American

191   Veterinary Medical Association's guidelines for humane euthanasia, for reasons unrelated to the

192   study. These horses were also determined to be free of orthopedic disease based on pre-mortem

193   physical examination and post mortem gross examination of the joint. The tissue was

194   transported, minced and digested as described above. Cells were recovered through

195   centrifugation, the supernatant decanted and the cellular pellet re-suspended in 5mL of

196   supplemented DMEM. The cell solution was transferred to a 25mL tissue culture flask

197   containing 5mL of supplemented DMEM. Cells were grown in monolayer culture, under the

198   conditions described above, until the 4th cell passage had been reached.

199   *Dynamic Culture--* Fourteen 2% PPLA coated PGA scaffolds and fourteen 4% PPLA

200   coated PGA scaffolds were placed in separate 110mL vessel flasks of the rotating bioreactor

201   system containing 110mL of supplemented DMEM. The scaffolds were presoaked for 24 hours

202   in the bioreactor at 37°C, 5% CO_2, 95% humidity, prior to cell introduction. After this time it

203   was noted that the scaffolds were floating at the apex of the flasks. Using sterile surgical

204   technique, scaffolds were sterily removed from the flasks, pierced centrally, and strung on loops

205   of 3-0 nylon surgical suture with knots placed adjacent to the scaffolds to prevent bunching on

206   the line. Seven scaffolds were placed per suture. The strings of scaffolds were then placed back

207   in to the bioreactors and presoaked for another 12 hours, at which time complete hydration and

208   submersion were achieved (Fig. 5).

209   Scaffolds were then dynamically seeded. Synovial membrane cells were removed from

210   the tissue culture flasks using as described above and counted using the Trypan Blue exclusion

211   assay(Strober 2001). Cells were added to the bioreactor flasks at a concentration of 475,000

212   cells per mL.

213   For the duration of culture, the bioreactor was maintained at 37°C, 5% CO_2, 95%

214   humidity at 51.1 rpm. Fifty percent of the cell culture medium volume was changed using sterile

215 technique every 3 days. Seven scaffolds were harvested on day 10 of culture, and 7 scaffolds

216 were harvested on day 21 of culture.

217 *Determination of Cell Viability*-- Cell viability was determined with the use of ethidium

218 homodimer-1 (4ul/ml PBS) and Calcein AM (Acetoxymethylester) (0.4ul/ml PBS) fluorescent

219 stains (Invitrogen, Carlsbad CA) and the use of Confocal Laser Microscopy. The Confocal Laser

220 Microscope consists of the BioRad Radiance 2000 confocal system coupled to an inverted

221 microscope (Olympus IX70 Olympus, Melville, NY) equipped with Krypton-Argon and red

222 diode laser. Approximately 1.0 mm sections were made from the halved scaffold using a rotary

223 paper cutter. A section from each scaffold's cut center and a section from each scaffold's

224 periphery was examined. Sections were incubated with the staining agents for 30 minutes at

225 room temperature, placed on a glass microscope slide, moistened with several drops of PBS, and

226 stained using the fluorescent double labeling technique. The sections were examined under 10x

227 magnification. Images were taken of each specimen as described above, (three from the section

228 periphery and three from the section center) at the 2 o'clock, 6o'clock and 10o'clock positions.

229 Images were digitally captured as described above. Live and dead cell counts were determined

230 by hand counts.

231 *DNA Quantification* -- One half of each construct was lyophilized and a dry weight

232 obtained. Samples were incubated in 1.0ml Papain Solution (2mM Dithiothreitol and 300ug/ml

233 Papain) at 60ºC in a water bath for 12 hours. A double stranded DNA quantification assay

234 (Quant-iT PicoGreen^{TM} Invitrogen, Carlsbad, CA) was performed. Double stranded DNA

235 extracted from bovine thymus was mixed with TE buffer (Invitrogen, Carlsbad, CA) to create

236 standard DNA concentrations of 1,000, 100, 10, and 1 ng/mL. The standards and 100uL of each

237 papain digested sample (used in the above GAG and hydroxyproline assays) were added to a

238   black 96 well plate. 100uL of 2ug/mL of Pico Green reagent was added to each well and the

239   plate was incubated for 5 minutes. Sample fluorescence was read at 485nm excitation/ 528nm

240   emission by a spectrophotometric plate reader (Synergy HT – KC-4, BioTek, Winooski, VT).

241   Absorbances were converted to ng/mL concentrations and total double stranded DNA yield in ng

242   using FT4 software (BioTek, Winooski, VT).

243   *Statistical Methods*— Data were tested for normality using a Shapiro-Wilk test. Scaffold

244   weights were compared using a 2-tailed paired t-test. Scaffold dsDNA content was analyzed

245   using a repeated- measures analysis of variance with a Geisser-Greenhouse correction.

246   Significance was set at $p < 0.05$. All statistical analyses were performed using a statistical

247   software program, (GraphPad Prism Version 6, San Diego, CA).

248

249   **Results**

250   *Experiment 1:*

251   As determined by the Trypan Blue exclusion assay, viability of cells at the time of

252   transfer from monolayer culture to static or dynamic seeding was 98.6%. No live cells were

253   detected in any of the media changes for either static or dynamically cultured scaffolds,

254   indicating that viable cells rapidly adhered to the scaffolds.

255   At the time of harvest upon gross examination, the fibers of the PGA scaffolds and the

256   sponge surface of the OPLA scaffolds were still visible. PGA scaffolds subjectively appeared

257   more translucent.

258   Despite equal cell seeding concentrations, the effect of dynamic bioreactor culture on cell

259   content of PGA scaffolds (PGA-D versus PGA-S) was to increase scaffold cellularity (P<0.001).

260   This was also found in OPLA-D versus OPLA-S scaffolds (P=0.028). The effect of scaffold type

261   also significantly increased scaffold cellularity of PGA-D versus OPLA-D (P=0.017), while

262   OPLA-S had great cellularity than PGA-S (P=0.0217; Table 1).

263   All groups, with the exception of OPLA-S, showed increased cellular distribution to the

264   periphery of the scaffolds (Table 2). Due to the shape of the OPLA-S on histological sectioning,

265   there was overlap of central and peripheral fields of view, precluding accurately localized cell

266   counts; peripheral cell count was 307 ±52 and central cell count was 287 ± 80 (P<0.464). Cells

267   grew in whorls, strands, and sheets on the PGA scaffolds, while cells grew in clumps on the

268   surface pores of the OPLA sponges (Fig. 6).

269   Staining for collagen and gycosaminoglycan using Masson's Trichrome and Safranin-O,

270   respectively, was negative for extracellular matrix production in all sections of all scaffold types

271   and culture conditions evaluated.

272   In the PGA-D group, the dimethylmethylene blue assay detected a mean of 22.29 µg of GAG

273   per scaffold, (range 19.34- 28.13µg), with a mean % GAG scaffold content of 0.0345% (µg

274   GAG per µg scaffold wet weight). No GAG was detected in OPLA constructs or PGA-S

275   constructs. The hydroxyproline assay did not detect collagen production in any group.

276

277   ***Experiment 2:***

278   Post PLLA modification, mean scaffold dry weights before soaking and seeding were

279   1.01mg for 2% PLLA coating and 1.52mg for 4% PLLA coating (P<0.001). Scaffold dry

280   weights decreased over time. Mean lyophilized weight on day 10 for 2% PLLA coating was

281   0.533mg, which decreased to 0.257mg on day 21 (P=0.02). Mean lyophilized weight on day 10

282   for 4% PLLA coating was 0.481mg, which decreased to 0.381mg on day 21 (P=0.043).

283   Scaffold cellularity as measured by dsDNA content increased over time: for the 2%

284   group, day 10 cellularity was 102.6 ng dsDNA/mg dry weight, and on day 21 it was 281.79

285   (P=0.021). On day 10 for the 4% group, dsDNA content was 111.01 ng dsDNA/mg dry weight

286   and on day 21 it was 140.2ng dsDNA/mg dry weight (P= 0.032; Fig. 7).

287   PLLA coating also affected scaffold dsDNA content. Scaffolds with the 2% PLLA

288   coating had greater dsDNA content than the 4% PLLA coating on day 21 (P=0.003), but not on

289   day 10 (P=0.602; Fig 7).

290   As visible under confocal microscopy, cells only adhered to the surface of exposed PGA

291   fibers and had poor to no penetration to the scaffold centers in all PLLA coated scaffolds. Viable

292   cell numbers were estimated only because of the marked cellular clumping; all scaffolds showed

293   mixtures of viable and non- viable cells localized in clumps on the scaffold outer margins (Figs

294   8-11). Histologic examination of H+E stained constructs revealed minimal cellular adhesion to

295   the PLLA, in all groups at all times, with cells growing primarily on the exposed PGA scaffold,

296   in tightly packed clumps, or adhering to exposed fibers of PGA. No extracellular matrix was

297   observed in any scaffolds on histologic analysis, which also reflected the uneven cellularity (Fig

298   12).

299

300   **Discussion:**

301   The current study analyzed the effect of scaffold type, biomechanical stimuli, and culture

302   duration on FLS seeding and production of specific meniscal ECM constituents. We found that

303   FLS-seeded PGA constructs cultured in a rotating bioreactor had the highest cellularity, with a

304   mean sulfated glycosaminoglycan content of 22.3µg per scaffold. PGA constructs cultured in

305   static conditions had the lowest cellularity. For PLLA coated PGA, increasing concentration of

306 PLLA decreased scaffold cellularity, while increased culture time increased scaffold cellularity,

307 as determined by the dsDNA assay. A non-uniform cellular distribution was observed for all

308 scaffold types and culture conditions.

309 Bioreactor culture provides a number of benefits over static culture, which would account for

310 the higher cellularity of PGA-D and OPLA-D versus PGA-S and OPLA-S scaffolds. The

311 rotating wall bioreactor used in this study provided a dynamic, laminar fluid shear, which

312 perfuses scaffold cultured cells (Bilodeau & Mantovani 2006), and thereby encourages cell

313 survival and proliferation by providing efficient transport of nutrients, gases, catabolites, and

314 metabolites and maintaining physiologic media pH (Gooch et al. 2001; Vunjak-Novakovic et al.

315 1998). Mixing of culture media also promotes cell seeding by creating matched relative

316 velocities of cells and scaffolds, particularly on non-woven PGA scaffolds (Vunjak-Novakovic et

317 al. 1998). In addition, the rotating wall bioreactor limits cellular stress by reducing strong shear

318 forces and cellular impact on the walls of the bioreactor (Bilodeau & Mantovani 2006).

319 However, in our study, scaffold characteristics such as scaffold density and hydrophilicity may

320 have negated the advantages of bioreactor culture, as seen with OPLA or PLLA coated scaffolds,

321 which had fewer cells and markedly uneven cell distribution, respectively.

322 A higher cell count was found on PGA-D versus OPLA-D, indicating either better adherence

323 or cell proliferation on PGA. Non-woven PGA scaffolds favor cellular capture and retention

324 because of their polar surface properties and high surface area for cellular adhesion (Day et al.

325 2004; Moran et al. 2003). Cellularity of PGA-D was further increased by the open weave and

326 low density (45-77mg/cc) of PGA scaffolds supports cellular proliferation through superior flow-

327 through of culture media and nutrient delivery (Vunjak-Novakovic et al. 1998). This is in

328 contrast to the highly dense (871mg/cc) OPLA sponges with non-communicating pores, which

329   could inhibit nutrient and gas transfer to seeded cells (Pazzano et al. 2004; Pazzano et al. 2000;

330   Wu et al. 1999). For PLLA covered PGA scaffolds, cells were located primarily on exposed

331   PGA fibers, and scaffold cellularity was inversely proportional to the concentration of PLLA.

332   Although PLLA is widely used in tissue-engineering applications because of its slower

333   degradation characteristics, strength, and mechanical properties, its hydrophobic, inert nature can

334   affect cell-matrix interactions and decrease cellular adhesion (Moran et al. 2003). While the

335   PLLA coating of PGA scaffolds was intended to protect from premature scaffold dissolution, we

336   observed that with longer duration of culture, scaffolds appeared to be more fragile to disruption

337   with forceps manipulation, particularly on the outer edges as well as around the centrally placed

338   suture. In agreement with this observation, all scaffold dry weights dropped over time,

339   indicating scaffold dissolution. Thus PLLA did not prevent PGA hydrolysis and decreased

340   scaffold integrity. PLLA coating also provided a hydrophobic barrier to centralized cell seeding

341   and ingrowth. Thus, for the future study of scaffold seeded equine FLS, use of PLLA type

342   scaffolds is not recommended.

343   Cell distribution across all scaffolds was uneven, in contrast to previous reports on bioreactor

344   chondrocyte culture (Mahmoudifar et al. 2005; Pazzano et al. 2004). Lower central cell density

345   in our scaffolds may have indicated poor axial cell penetration and in-growth. Alternatively,

346   higher peripheral cellularity could reflect increased peripheral cell division caused by increased

347   exposure to media nutrients, gas exchange, and mechanotransductive effects (Mahmoudifar et

348   al. 2002). Additionally the OPLA scaffolds had clumped cell distribution in the outermost pores.

349   The OPLA sponge porosity may not allow uniform cell distribution; the 100-200μm pores do not

350   consistently communicate with each other. While OPLA-S did not have different peripheral and

351   central cell counts, this was due to an artifact of the sponge shape and precluded distinction of

352   peripheral cells from central cells. To increase central scaffold cell content, flow-through

353   bioreactors (Bilodeau & Mantovani 2006) may have greater cell seeding efficiencies than rotary

354   bioreactors. Alternatively, cells may be seeded at the time of scaffold formation, such as during

355   hydrogel synthesis, to insure central scaffold cellularity (Narita et al. 2009).

356   The culture conditions utilized in the present study resulted in minimal to no ECM formation,

357   in contrast to other studies. The mean GAG content of the PGA-D scaffold of 0.0345% (wet

358   weight basis) was lower than the 0.6-0.8% wet weight in the normal meniscus, and thus

359   represents a sub- optimal response for engineering purposes (AufderHeide & Athanasiou 2004).

360   Synoviocytes typically produce collagen type I constitutively, (Garner & al. 2000; Levick 1996),

361   however production and deposition of hydroxyproline was not detected in this study. The most

362   likely reason for this failure of ECM formation was lack of culture with a specific

363   fibrochondrogenic media. For example, culture with recombinant transforming growth factor-

364   beta, insulin-like growth factor -1 and basic fibroblast growth factor have been shown to induce

365   *in vitro* collagen formation in human synoviocytes (Pei et al. 2008). However, treatment of

366   equine FLS with the same recombinant chondrogenic growth factors, in the same culture

367   conditions as the present study, also failed to produce measureable ECM (Fox et al. 2009).

368   Reported scaffold seeding concentrations for cartilage tissue engineering include 30,000

369   fibroblasts/mL (Day et al. 2004); 600,000 chondrocytes/mL (Stading M & R 1999); 5 million

370   chondrocytes/ mL (Griffon et al. 2005); and 10 million chondrocytes/mL (Hu et al. 2005). Our

371   seeding density of 1 million equine FLS per scaffold may have been too low, as dense cell

372   aggregates are required for meniscal developmental fibrochondrogenesis (Clark & Ogden 1983)

373   due to the embryonic community effect (Gurdon et al. 1993). In the present study the FLS were

374   exposed to the mild shear forces and hydrostatic pressurization in a rotating bioreactor (Mauck et

375   al. 2002) which may not have been the optimal type of forces required for synovial collagen I

376   formation. A combination of in vitro tensile and compressive forces(AufderHeide &

377   Athanasiou 2004; Benjamin & Ralphs 1998) may be required to support formation GAG

378   (Valiyaveettil et al. 2005) and types I and II collagen (Kambic & McDevitt 2005), the major

379   ECM components of fibrocartilage. Cell culture on scaffolds may also result in cellular stress

380   shielding, thereby resulting in suboptimal matrix formation (Huey & Athanasiou 2011).

381   Increased culture time may also be beneficial to ECM formation; other studies show time

382   dependent ECM expression (Griffon et al. 2005; Mueller et al. 1999; Sha'ban et al. 2008). One

383   study of synovial chondrogenesis on PGA scaffolds utilized a longer culture duration of 60 days,

384   with successful ECM formation (Sakimura et al. 2006). Despite better cellularity, PGA scaffolds

385   began loosing integrity over the culture period, even when coated with PLLA. Unless rapid ECM

386   formation can be achieved before dissolution occurs, PGA hydrolyzes too quickly (t1/2 =16

387   days) for the purpose of long term meniscal fibrocartilage synthesis. Treatment with

388   chondrogenic or fibrochondrogenic media may induce production of ECM, thus making the

389   culture systems described here more feasible for meniscal tissue engineering.

390   **Conclusion:**

391   In conclusion, we reject the null hypothesis; dynamic cell seeding and culture, as well as

392   increased culture duration, increased scaffold cellularity. Scaffold type also affected cellularity;

393   for bioreactor culture, PGA had higher cell counts versus OPLA, while OPLA had higher cell

394   counts versus PGA in static culture. Cells could only grow unevenly in the pores of the OPLA

395   sponge, and cells could not adhere to the PLLA coating of PGA scaffolds. Increasing the

396   concentration of PLLA coating on a PGA scaffold decreased the cellularity of the scaffold, and

397   did not prevent scaffold dissolution. While PGA culture in a bioreactor produced measureable

398   GAG, no culture technique produced visible collagen. For this reason, and due to the dissolution

399   of PGA scaffolds, the exact culture of conditions described here are not recommended for

400   inducing equine fibrochondrogenesis towards meniscal tissue engineering. Further research is

401   recommended to enhance extracellular matrix production through additional biomechanical and

402   biological stimulation, including treatment with chondrogenic media, increased culture duration,

403   and increased cell seeding concentrations.

404

407

408

References

409

410

411   **Amin M, Kurosaki M, Watanabe T, Tanaka S, and Hori T. 2000. A comparative study of**
412   **MIB-1 staining indices of gliomas measured by NIH Image analysis program and**
413   **conventional manual cell counting method. *Neurologic Research* 22:495-500.**

414   **Arnoczky SP, and Warren RF. 1983. The microvasculature of the meniscus and its**
415   **response to injury. An experimental study in the dog. *Am J Sports Med* 11:131-141.**

416   **AufderHeide AC, and Athanasiou KA. 2004. Mechanical stimulation toward tissue**
417   **engineering of the knee meniscus. *Ann Biomed Eng* 32:1161-1174.**

418   **Aufderheide AC, and Athanasiou KA. 2005. Comparison of scaffolds and culture**
419   **conditions for tissue engineering of the knee meniscus. *Tissue Eng* 11:1095-1104.**

420   **Beatty MW, Ojha AK, Cook JL, Alberts LR, Mahanna GK, Iwasaki LR, and Nickel JC.**
421   **2002. Small intestinal submucosa versus salt-extracted polyglycolic acid-poly-L-**
422   **lactic acid: a comparison of neocartilage formed in two scaffold materials. *Tissue***
423   ***Eng* 8:955-968.**

424   **Benjamin M, and Ralphs JR. 1998. Fibrocartilage in tendons and ligaments--an adaptation**
425   **to compressive load. *J Anat* 193 (Pt 4):481-494.**

426   **Benzinou A, Hojeij Y, and Roudot A. 2005. Digital image analysis of haematopoietic**
427   **clusters. *Computational Methods and Programs in Biomedicine* 77:121-127.**

428   **Bilodeau K, and Mantovani D. 2006. Bioreactors for Tissue Engineering: Focus on**
429   **Mechanical Constraints. A Comparative Review. *Tissue Eng*12:2367-83.**

430   **Burks RT, Metcalf MH, and Metcalf RW. 1997. Fifteen-year follow-up of arthroscopic**
431   **partial meniscectomy. *Arthroscopy* 13:673-679.**

432   **Cisa J, Basora J, Madarnas P, Ghibely A, and Navarro-Quilis A. 1995. Meniscal repair by**
433   **synovial flap transfer. Healing of the avascular zone in rabbits. *Acta Orthop Scand***
434   **66:38-40.**

435   **Clark CR, and Ogden JA. 1983. Development of the menisci of the human knee joint.**
436   **Morphological changes and their potential role in childhood meniscal injury. *J Bone***
437   ***Joint Surg Am* 65:538-547.**

438   **Cox JS, Nye CE, Schaefer WW, and Woodstein IJ. 1975. The degenerative effects of partial**
439   **and total resection of the medial meniscus in dogs' knees. *Clin Orthop Relat Res***
440   **109:178-183.**

441   **Davisson T, Sah R, and Ratcliffe A. 1999. Perfusion increases cell content and matrix**
442   **synthesis in chondrocyte three- dimensional cultures. *Tissue Eng* 8:807-816.**

443   **Day R, Boccaccini A, and Shurey A. 2004. Assessment of polyglycolic acid mesh and**
444   **bioactive glass for soft tissue engineering scaffolds.** *Biomaterials* **25:5857-5864.**

445   **De Bari C, Dell'Accio F, Tylzanowski P, and Luyten FP. 2001. Multipotent mesenchymal**
446   **stem cells from adult human synovial membrane.** *Arthritis Rheum* **44:1928-1942.**

447   **Esposito AR, Moda M, Cattani SM, de Santana GM, Barbieri JA, Munhoz MM, Cardoso**
448   **TP, Barbo ML, Russo T, D'Amora U. 2013. PLDLA/PCL-T Scaffold for Meniscus**
449   **Tissue Engineering.** *Biores Open Access* **2:138-147.**

450   **Farndale RW, Buttle DJ, and Barrett AJ. 1986. Improved quantitation and discrimination**
451   **of sulphated glycosaminoglycans by use of dimethylmethylene blue.** *Biochim*
452   *Biophys Acta* **883:173-177.**

453   **Fithian DC, Kelly MA, and Mow VC. 1990. Material properties and structure-function**
454   **relationships in the menisci.** *Clin Orthop Relat Res* **252:19-31.**

455   **Fox DB, Warnock JJ, Stoker AM, Luther JK, and Cockrell M. 2009. Effects of growth**
456   **factors on equine synovial fibroblasts seeded on synthetic scaffolds for avascular**
457   **meniscal tissue engineering.** *Res Vet Sci* **88:326-32.**

458   **Garner P. 2000. Molecular basis and clinical use of biochemical markers of bone, and**
459   **synovium in joint disease.** *Arthritis and Rheumatism* **43:953.**

460   **Girman P, Kriz J, Friedmansky J, and Saudek F. 2003. Digital imaging as a possible**
461   **approach in evaluation of islet yield.** *Cell Transplantation* **12:129-133.**

462   **Goedkoop A, Rie Md, Teunissen M, and 297:51-59 eaADR. 2005. Digital image analysis for**
463   **the evaluation of the inflammatory infiltrate in psoriasis.** *Archives of Dermatological*
464   *Research* **297:51-59.**

465   **Gooch KJ, Kwon JH, Blunk T, Langer R, Freed LE, and Vunjak-Novakovic G. 2001.**
466   **Effects of mixing intensity on tissue-engineered cartilage.** *Biotechnol Bioeng* **72:402-**
467   **407.**

468   **Griffon D, Sedighi M, Sendemir-Urkmez A, and al. e. 2005. Evaluation of vacuum and**
469   **dynamic cell seeding of polyglycolic acid and chitosan scaffolds for cartilage**
470   **engineering.** *American Journal of Veterinary Research* **66:599-605.**

471   **Gunja NJ, and Athanasiou KA. 2010. Additive and synergistic effects of bFGF and hypoxia**
472   **on leporine meniscus cell-seeded PLLA scaffolds.** *J Tissue Eng Regen Med* **4:115-**
473   **122.**

474   **Gurdon JB, Lemaire P, and Kato K. 1993. Community effects and related phenomena in**
475   **development.** *Cell* **75:831-834.**

476   **Hee CK, Jonikas MA, and Nicoll SB. 2006. Influence of three-dimensional scaffold on the**
477   **expression of osteogenic differentiation markers by human dermal fibroblasts.**

478   *Biomaterials* **27:875-884.**

479   **Hu J, Athaasiou K, and al. e. 2005. Low density cultures of bovine chondorcytes: effects of**
480   **scaffold material and culture system.** *Biomaterials* **26:2001-2012.**

481   **Huey DJ, and Athanasiou KA. 2011. Maturational growth of self-assembled, functional**
482   **menisci as a result of TGF-beta1 and enzymatic chondroitinase-ABC stimulation.**
483   *Biomaterials* **32:2052-2058.**

484   **Imler SM, Doshi AN, and Levenston ME. 2004. Combined effects of growth factors and**
485   **static mechanical compression on meniscus explant biosynthesis.** *Osteoarthritis*
486   *Cartilage* **12:736-744.**

487   **Ionescu LC, and Mauck RL. 2013. Porosity and cell preseeding influence electrospun**
488   **scaffold maturation and meniscus integration in vitro.** *Tissue Eng Part A* **19:538-**
489   **547.**

490   **Kambic HE, and McDevitt CA. 2005. Spatial organization of types I and II collagen in the**
491   **canine meniscus.** *J Orthop Res* **23:142-149.**

492   **Kang SW, Son SM, Lee JS, Lee ES, Lee KY, Park SG, Park JH, and Kim BS. 2006.**
493   **Regeneration of whole meniscus using meniscal cells and polymer scaffolds in a**
494   **rabbit total meniscectomy model.** *J Biomed Mater Res A* **77:659-671.**

495   **Kim B, Putnam A, Kulik J, and al. e. 1998. Optimizing seeding and culture methods to**
496   **engineer smooth muscle tissue on biodegradable polymer matricies.** *Biotechnology*
497   *and Bioengineering* **57:46-54.**

498   **Kobayashi K, Fujimoto E, Deie M, Sumen Y, Ikuta Y, and Ochi M. 2004. Regional**
499   **differences in the healing potential of the meniscus-an organ culture model to**
500   **eliminate the influence of microvasculature and the synovium.** *Knee* **11:271-278.**

501   **Kobuna Y, Shirakura K, and Niijima M. 1995. Meniscal repair using a flap of synovium.**
502   **An experimental study in the dog.** *Am J Knee Surg* **8:52-55.**

503   **Lavik E, Teng YD, Snyder E, and Langer R. 2002. Seeding neural stem cells on scaffolds of**
504   **PGA, PLA, and their copolymers.** *Methods Mol Biol* **198:89-97.**

505   **Levick JR, Price FM, Mason FM. 1996.** *Synovial matrix—synovial fluild systems of joints.*
506   **In: WD Comper (ed): Extracellular Matrix. Amsterdam: Harwood Academic**
507   **Publishers, 235-252.**

508   **Loukas CG, Wilson GD, Vojnovic B, and Linney A. 2003. An image analysis-based**
509   **approach for automated counting of cancer cell nuclei in tissue sections.** *Cytometry A*
510   **55:30-42.**

511   **Mahmoudifar N, Doran P, and al. e. 2005. Tissue engineering human cartilage in**
512   **bioreactors using single and composite cell seeded scaffolds.** *Biotechnology and*

513   *Bioengineering* **91:338-355.**

514   **Mahmoudifar N, Sikavistas V, Bancroif G, and Mikko A. 2002. Formation of three**
515   **dimensional cell/ polymer constructs for bone tissue engineering in a spinner flask**
516   **and a rotating wall vessel bioreactor.** *Journal of Bimedical Material Research*
517   **62:136-148.**

518   **Mauck RL, Seyhan SL, Ateshian GA, and Hung CT. 2002. Influence of seeding density and**
519   **dynamic deformational loading on the developing structure/function relationships**
520   **of chondrocyte-seeded agarose hydrogels.** *Ann Biomed Eng* **30:1046-1056.**

521   **Moran J, Pazzano B, and Bonassar L. 2003. Characterization of polylactic acid –**
522   **polyglycolic acid composites for cartilage tissue engineering.** *Tissue Eng* **9:63-70.**

523   **Mueller SM, Shortkroff S, Schneider TO, Breinan HA, Yannas IV, and Spector M. 1999.**
524   **Meniscus cells seeded in type I and type II collagen-GAG matrices in vitro.**
525   *Biomaterials* **20:701-709.**

526   **Narita A, Takahara M, Ogino T, Fukushima S, Kimura Y, and Tabata Y. 2009. Effect of**
527   **gelatin hydrogel incorporating fibroblast growth factor 2 on human meniscal cells**
528   **in an organ culture model.** *Knee* **16:285-289.**

529   **Nishimura K, Solchaga LA, Caplan AI, Yoo JU, Goldberg VM, and Johnstone B. 1999.**
530   **Chondroprogenitor cells of synovial tissue.** *Arthritis Rheum* **42:2631-2637.**

531   **Ochi M, Mochizuki Y, Deie M, and Ikuta Y. 1996. Augmented meniscal healing with free**
532   **synovial autografts: an organ culture model.** *Arch Orthop Trauma Surg* **115:123-126.**

533   **Pazzano, Davisson, Seidel, Pei, Gray, and al e. 2004. Long term culture of tissue engineered**
534   **cartilage in a perfused chamber with mechanical stimulation.** *Biorheology* **41:445-**
535   **458.**

536   **Pazzano D, Mercier K, Moran J, and al. e. 2000. Comparison of chondrogenensis in static**
537   **and perfused bioreactor culture.** *Biotechnology Progress* **16:893-896.**

538   **Pei M, He F, and Vunjak-Novakovic G. 2008. Synovium-derived stem cell-based**
539   **chondrogenesis.** *Differentiation* **76:1044-1056.**

540   **Peroni JF, and Stick JA. 2002. Evaluation of a cranial arthroscopic approach to the stifle**
541   **joint for the treatment of femorotibial joint disease in horses: 23 cases (1998-1999).** *J*
542   *Am Vet Med Assoc* **220:1046-1052.**

543   **Reddy GK, and Enwemeka CS. 1996. A simplified method for the analysis of**
544   **hydroxyproline in biological tissues.** *Clin Biochem* **29:225-229.**

545   **Rodeo SA, Seneviratne A, Suzuki K, Felker K, Wickiewicz TL, and Warren RF. 2000.**
546   **Histological analysis of human meniscal allografts. A preliminary report.** *J Bone*
547   *Joint Surg Am* **82-A:1071-1082.**

548   Sakimura K, Matsumoto T, Miyamoto C, Osaki M, and Shindo H. 2006. Effects of insulin-
549   like growth factor I on transforming growth factor beta1 induced chondrogenesis of
550   synovium-derived mesenchymal stem cells cultured in a polyglycolic acid scaffold.
551   *Cells Tissues Organs* 183:55-61.

552   Sha'ban M, Kim SH, Idrus RB, and Khang G. 2008. Fibrin and poly(lactic-co-glycolic acid)
553   hybrid scaffold promotes early chondrogenesis of articular chondrocytes: an in vitro
554   study. *J Orthop Surg* 3:17.

555   Sherwood JK, Riley SL, Palazzolo R, Brown SC, Monkhouse DC, Coates M, Griffith LG,
556   Landeen LK, and Ratcliffe A. 2002. A three-dimensional osteochondral composite
557   scaffold for articular cartilage repair. *Biomaterials* 23:4739-4751.

558   Shirakura K, Niijima M, Kobuna Y, and Kizuki S. 1997. Free synovium promotes meniscal
559   healing. Synovium, muscle and synthetic mesh compared in dogs. *Acta Orthop Scand*
560   68:51-54.

561   Smith R, Dunlon B, Gupta, and al. e. 1995. Effects of fluid induced shear on articular
562   chondrocyte morphology and metabolism in vitro. *Journal of Orthopaedic Research*
563   13:824.

564   Stading M, and R L. 1999. Mechanical shear properties of cell-polymer cartilage
565   constructs. *Tissue Eng* 5:241-250.

566   Strober W. 2001. Trypan blue exclusion test of cell viability. *Curr Protoc Immunol*
567   Appendix 3:Appendix 3B.

568   Valiyaveettil M, Mort JS, and McDevitt CA. 2005. The concentration, gene expression, and
569   spatial distribution of aggrecan in canine articular cartilage, meniscus, and anterior
570   and posterior cruciate ligaments: a new molecular distinction between hyaline
571   cartilage and fibrocartilage in the knee joint. *Connect Tissue Res* 46:83-91.

572   Vunjak-Novakovic G, Obradovic B, Martin I, Bursac PM, Langer R, and Freed LE. 1998.
573   Dynamic cell seeding of polymer scaffolds for cartilage tissue engineering.
574   *Biotechnol Prog* 14:193-202.

575   Walmsley JP. 1995. Vertical tears of the cranial horn of the meniscus and its cranial
576   ligament in the equine femorotibial joint: 7 cases and their treatment by
577   arthroscopic surgery. *Equine Vet J* 27:20-25.

578   Walmsley JR, Phillips TJ, and Townsend HG. 2003. Meniscal tears in horses: an evaluation
579   of clinical signs and arthroscopic treatment of 80 cases. *Equine Vet J* 35:402-406.

580   Wu F, Dunkelman N, and Peterson A. 1999. Bioreactor development for tissue engineered
581   cartilage. *Annals of the New York Academy of Science* 875:405-411.

582

583 **Tables**
584
585 Table 1: The effect of seeding and cell culture biomechanical environment and the effect of
586 scaffold type on scaffold cellularity.

	Cell Count (Mean number of cells per 10x objective field ±SD)		Effect of biomechanical environment (dynamic vs static culture)
Scaffold type:	Biomechanical environment:		
	Dynamic culture	Static culture	
PGA	1128 ±575 cells	54 ±34 cells	P<0.001
OPLA	375 ±118 cells	301 ±65 cells	P= 0.028
Effect of scaffold type (PGA vs OPLA)	P=0.017	P=0.0217	

587

588 **Table 2:**
589 Peripheral and central cell count (Mean number of cells per 10x objective field ±SD).

Scaffold	Peripheral cell count	Central cell count	P- value
PGA-D	1433 ±487	724 ±314	P<0.001
PGA-S	80 ±28	28 ±11	P<0.001
OPLA-D	476 ±90	295 ±55	P<0.001

590
591

Figures

Figure 1. Rotating wall bioreactor flask (110mL) containing media and PGA scaffolds seeded with equine fibroblast-like synoviocytes (**A**). Flasks loaded on the rotating base apparatus; flasks rotate around their longitudinal axis (**B**).
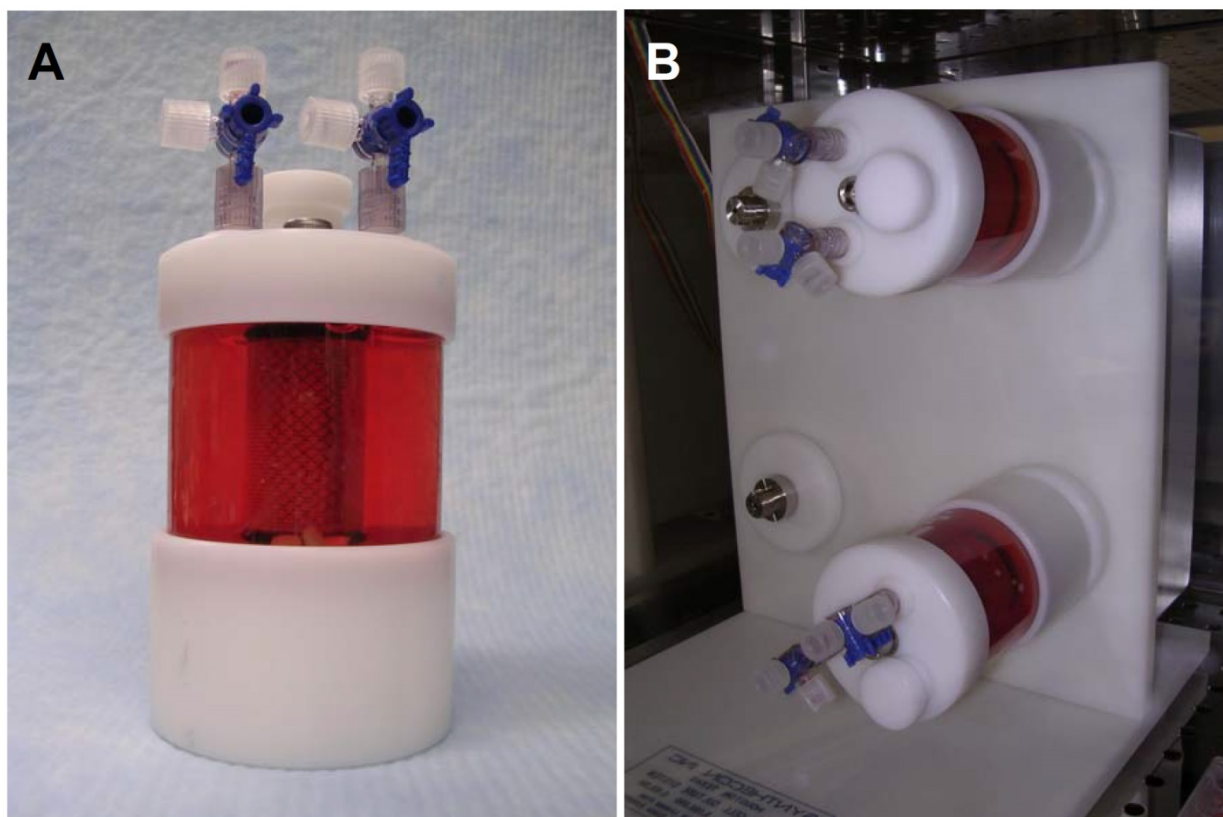
598   Figure 2. Static culture of equine fibroblast- like synoviocytes on PGA scaffolds in a 24 well

599   tissue culture plate, with each well containing 2mL of supplemented DMEM.

600
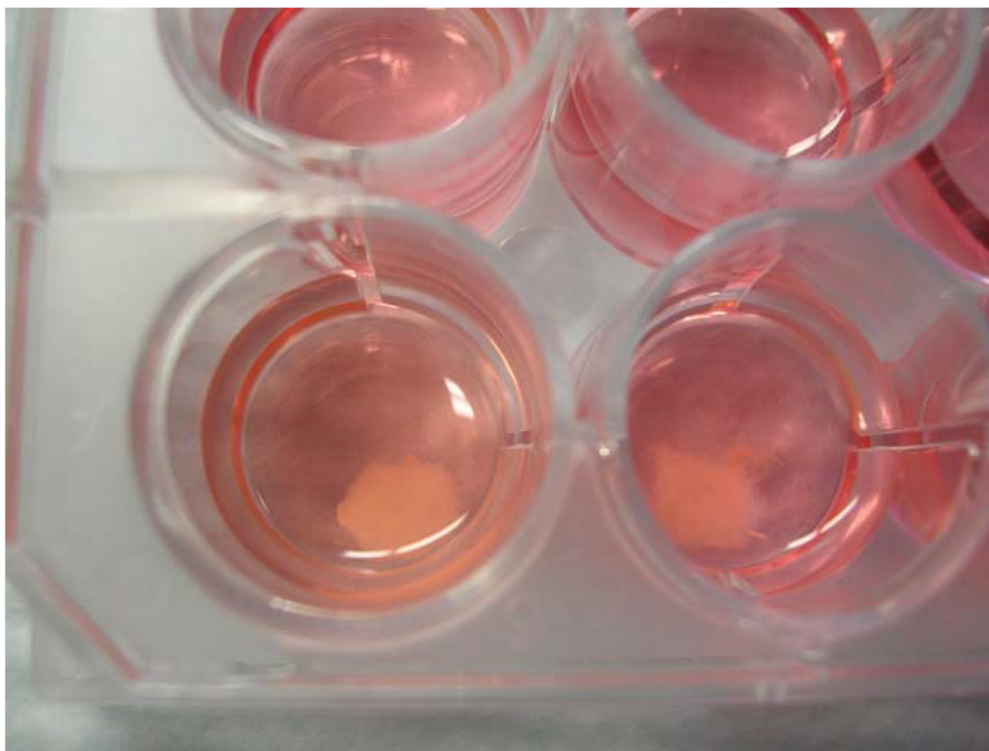
601

602

603

604   Figure 3. Method for viewing all scaffolds to standardize cell counts and determine regional cell

605   count differences between the scaffold center and periphery. Cells were counted at the periphery

606   and central regions (dark dotted circles) of each scaffold (cross- hatched circle) using digital

607   image analysis; peripheral cell counts (light dotted circles) were obtained at the 2o'clock,

608   6o'clock and 19o'clock positions. Circles represent a low power (10X objective) field of view.

609

610
611
612

613
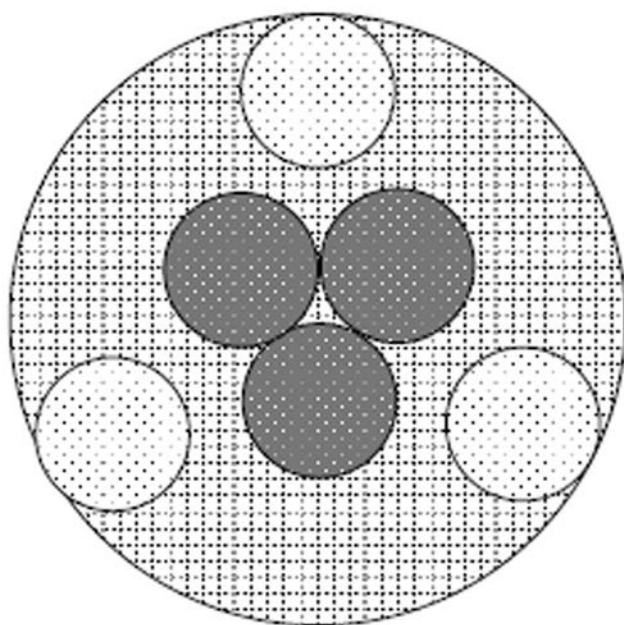
614   Figure 4. Scanning electron microscopy of a 2% PLLA coated PGA scaffold (**A**) and a 4%

615   PLLA coated scaffold (**B**) prior to cell seeding; bar = 100µm.

616

617
618
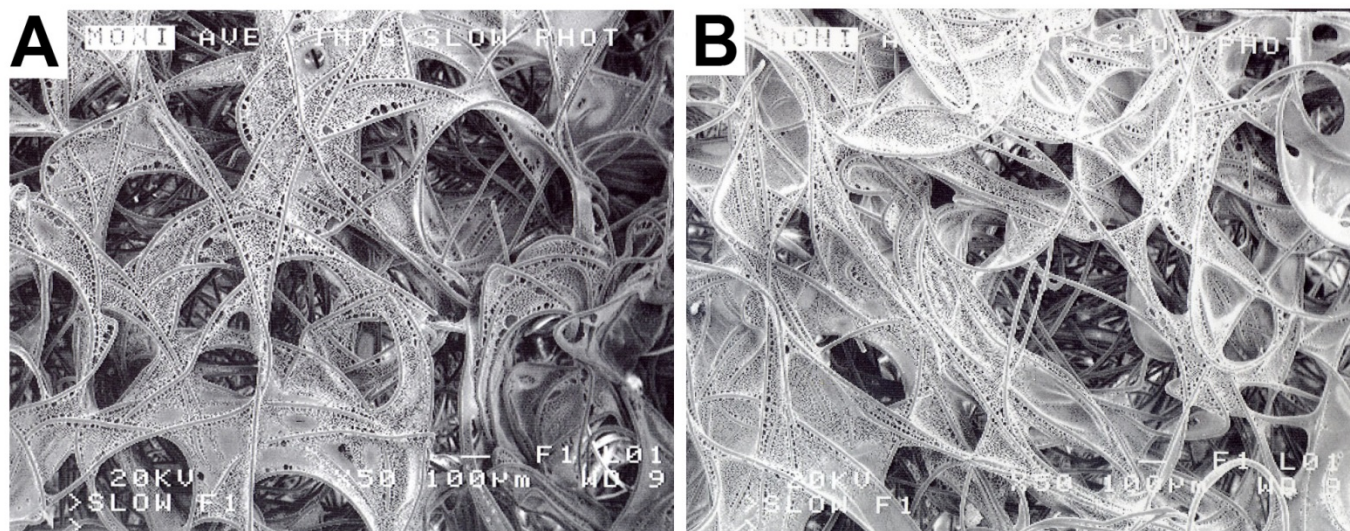
619

620 Figure 5. Rotating wall bioreactor flask containing 2% PLLA coated PGA scaffolds, strung on

621 suture to ensure equal submersion and positioning in the rotating flask.

622

623

624

625
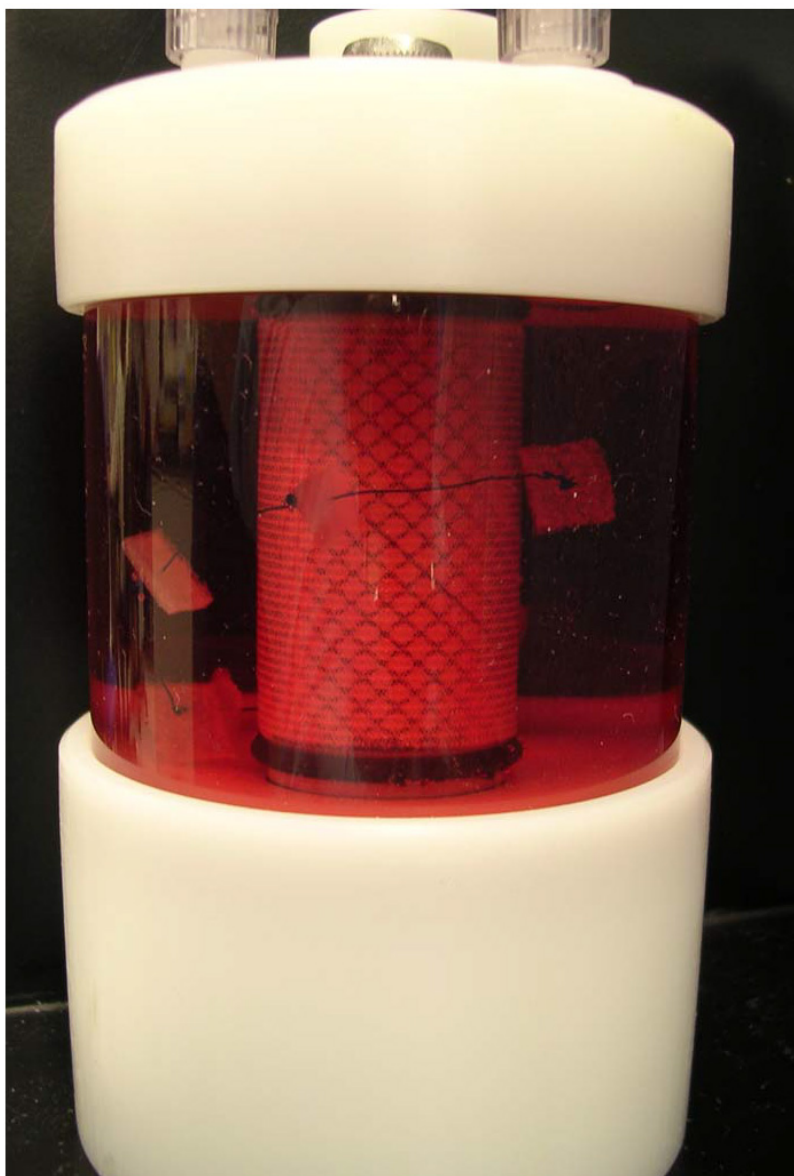
626   Figure 6. Micrographs of scaffolds seeded with equine fibroblast-like synoviocytes; Hematoxylin

627   and Eosin staining, 10x objective magnification; bar = 100µm. **A**) PGA scaffold cultured in a

628   static environment; **B**) PGA scaffold cultured in a dynamic environment (rotating bioreactor); **C**)

629   OPLA scaffold cultured in a dynamic environment (rotating bioreactor); **D**) OPLA scaffold

630   cultured in a static environment. Note the intact PGA fibers (open arrow) and the cells located in

631   clumps in the pores of the OPLA scaffold (closed arrows).

632

633
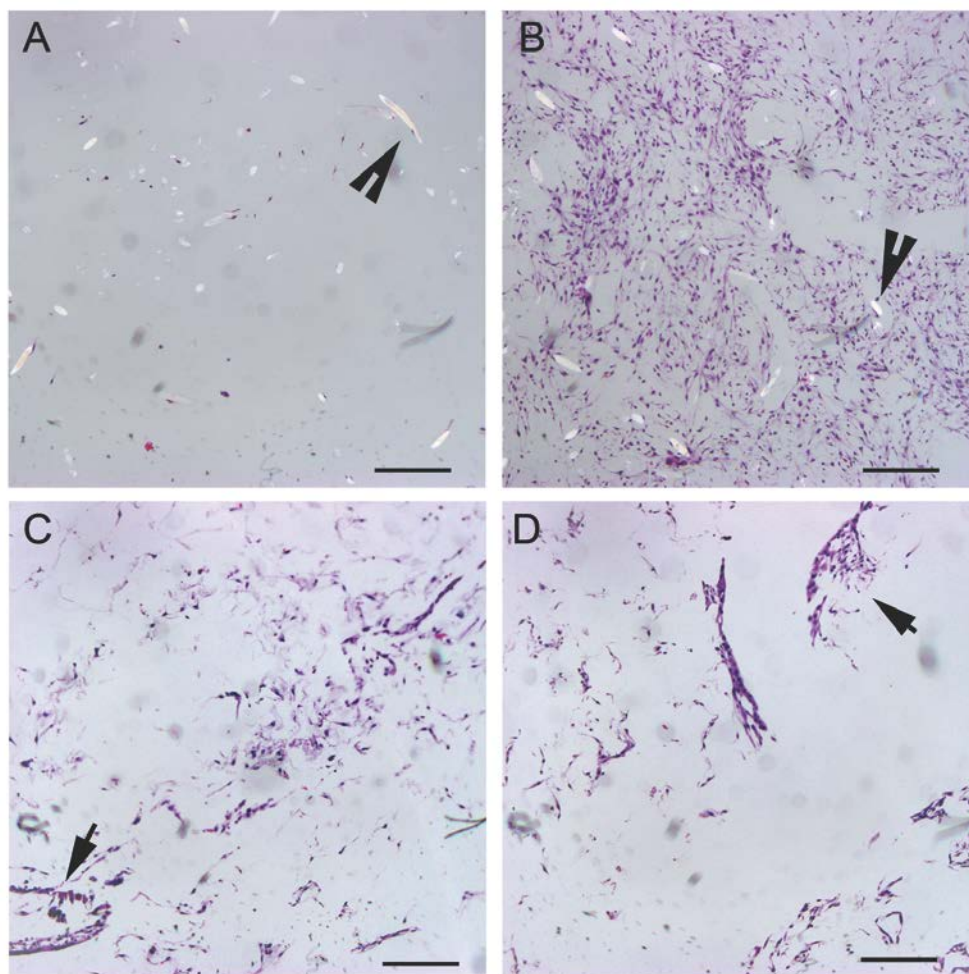
634

635   Figure 7. Mean ±Standard Error of the Mean (SEM) of dsDNA content of PGA scaffolds coated

636   in 2% PLLA and 4% PLLA, seeded dynamically and cultured in a rotating bioreactor for 14 days

637   and 21 days. A bar and (*) indicates a significant difference between two treatment
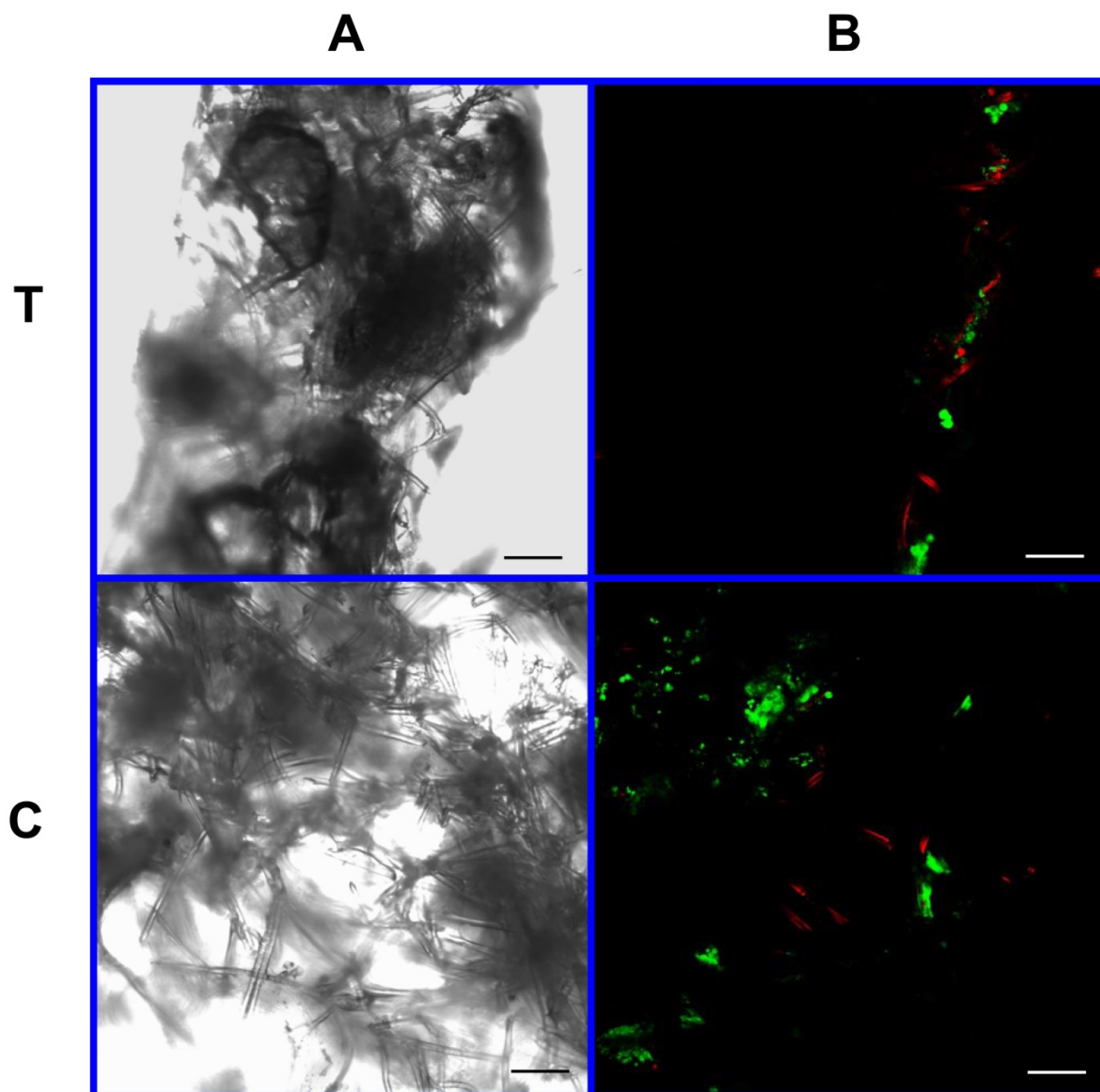
638   groups(P<0.05).

639

640
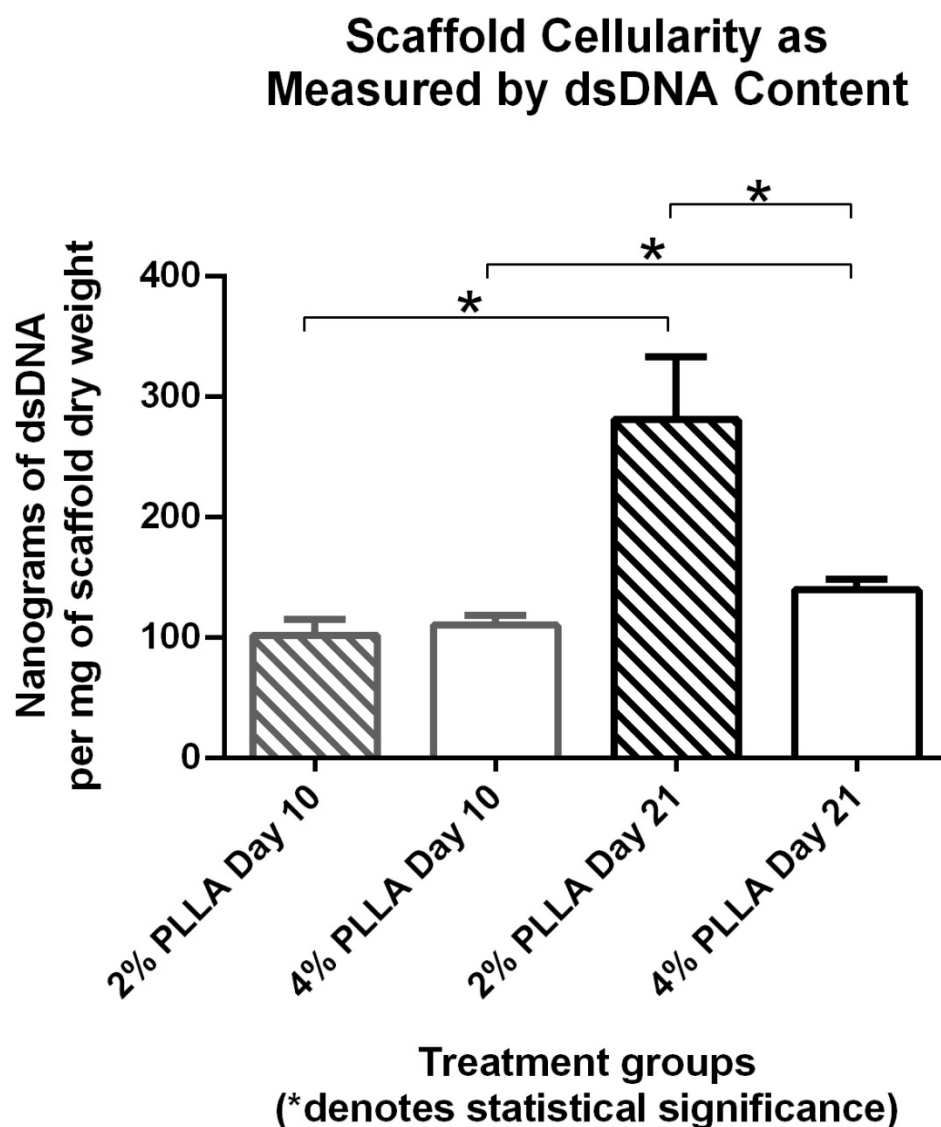
641

642   Figure 8. Photomicrographs of 2% PLLA coated PGA constructs harvested on day 10, under

643   standard light (column **A**) and under laser confocal microscopy (column **B**), using the calcein

644   AM-ethidium homodimer live-dead assay. Images represent scaffold transverse cross sections

645   (row **T**) and scaffold surface coronal sections (row **C**). Green stained cells are alive, red stained

646   cells are dead. 10x objective magnification; bar = 100µm.

647

648
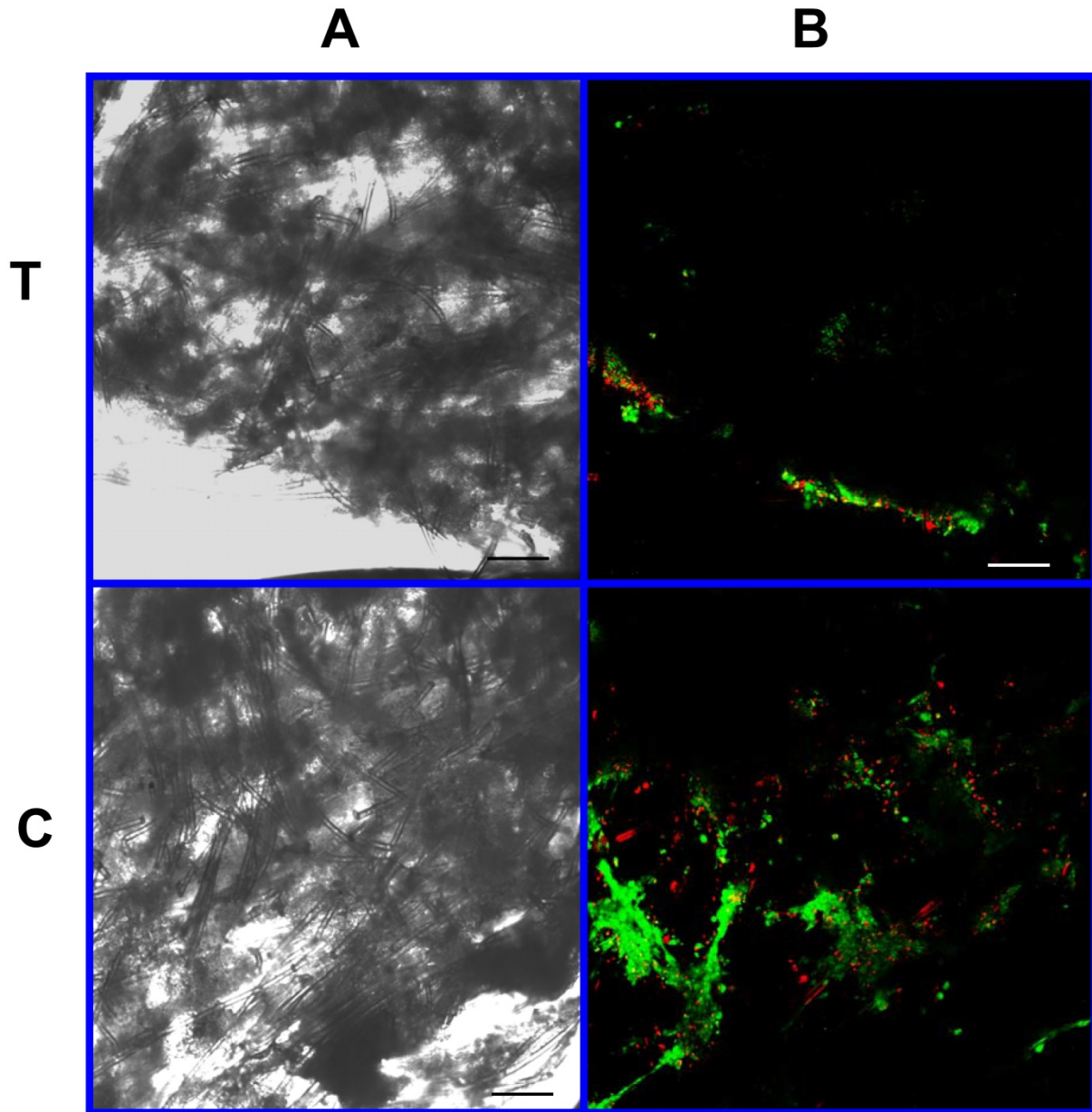
649 Figure 9. Photomicrographs of 2% PLLA coated PGA constructs harvested on day 21, under

650 standard light (column **A**) and under laser confocal microscopy (column **B**), using the calcein

651 AM-ethidium homodimer live-dead assay. Images represent scaffold transverse cross sections

652 (row **T**) and scaffold surface coronal sections (row **C**). Green stained cells are alive, red stained

653 cells are dead. Note the spurious red staining of scaffold PGA fibers. 10x objective

654 magnification; bar = 100μm.

655

656
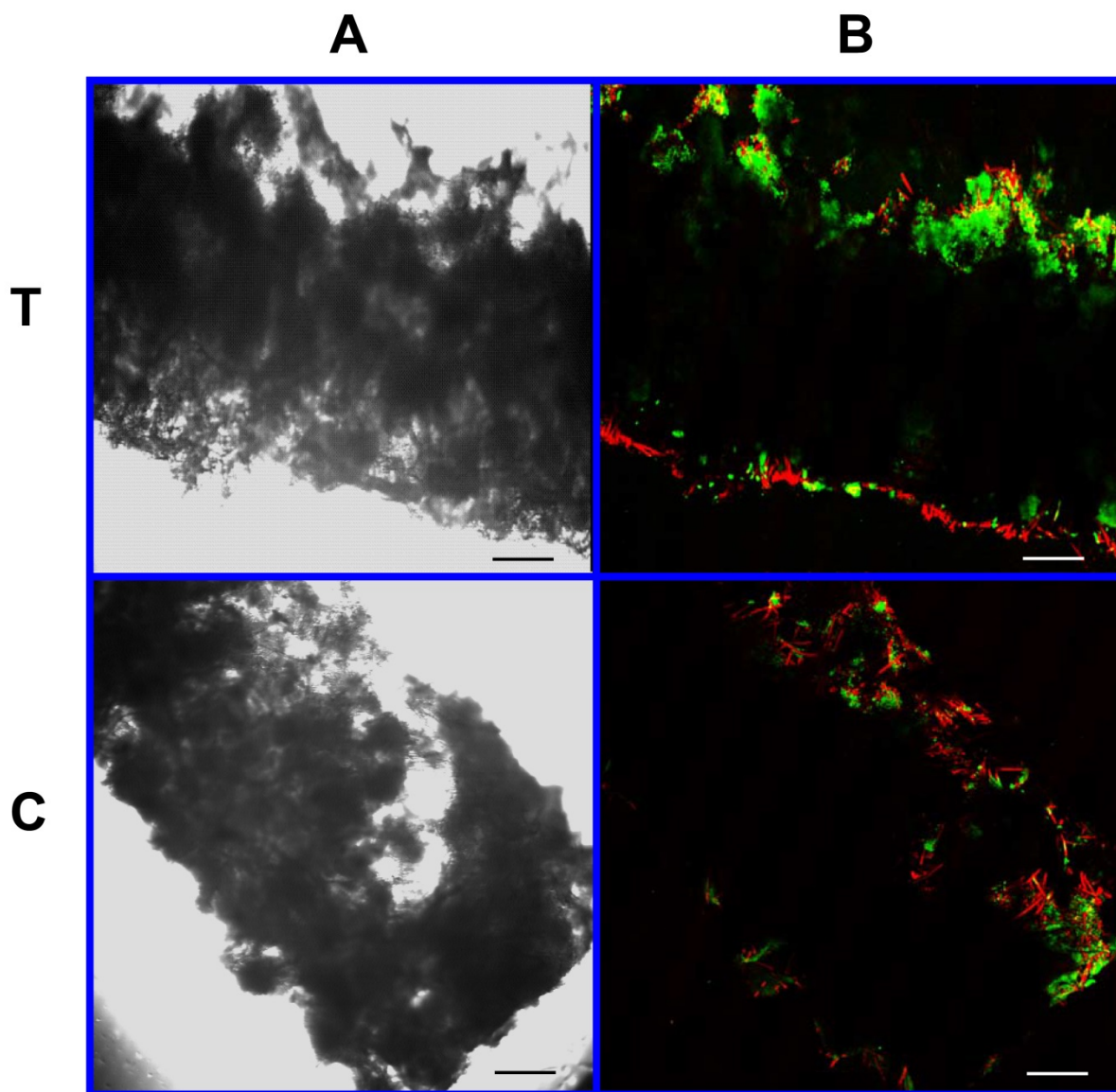
657 Figure 10. Photomicrographs of 4% PLLA coated PGA constructs harvested on day 10, under

658 standard light (column **A**) and under laser confocal microscopy (column **B**), using the calcein

659 AM-ethidium homodimer live-dead assay. Images represent scaffold transverse cross sections

660 (row **T**) and scaffold surface coronal sections (row **C**). Green stained cells are alive, red stained

661 cells are dead. Note the spurious red staining of PGA fibers. 10x objective magnification; bar =

662 100µm.

663

664

665

666 Figure 11. Photomicrographs of 4% PLLA coated PGA constructs harvested on day 21, under

667 standard light (column **A**) and under laser confocal microscopy (column **B**), using the calcein

668 AM-ethidium homodimer live-dead assay. Images represent scaffold transverse cross sections

669 (row **T**) and scaffold surface coronal sections (row **C**). Green stained cells are alive, red stained

670 cells are dead. Note the spurious red staining of PGA fibers.10x objective magnification; bar =
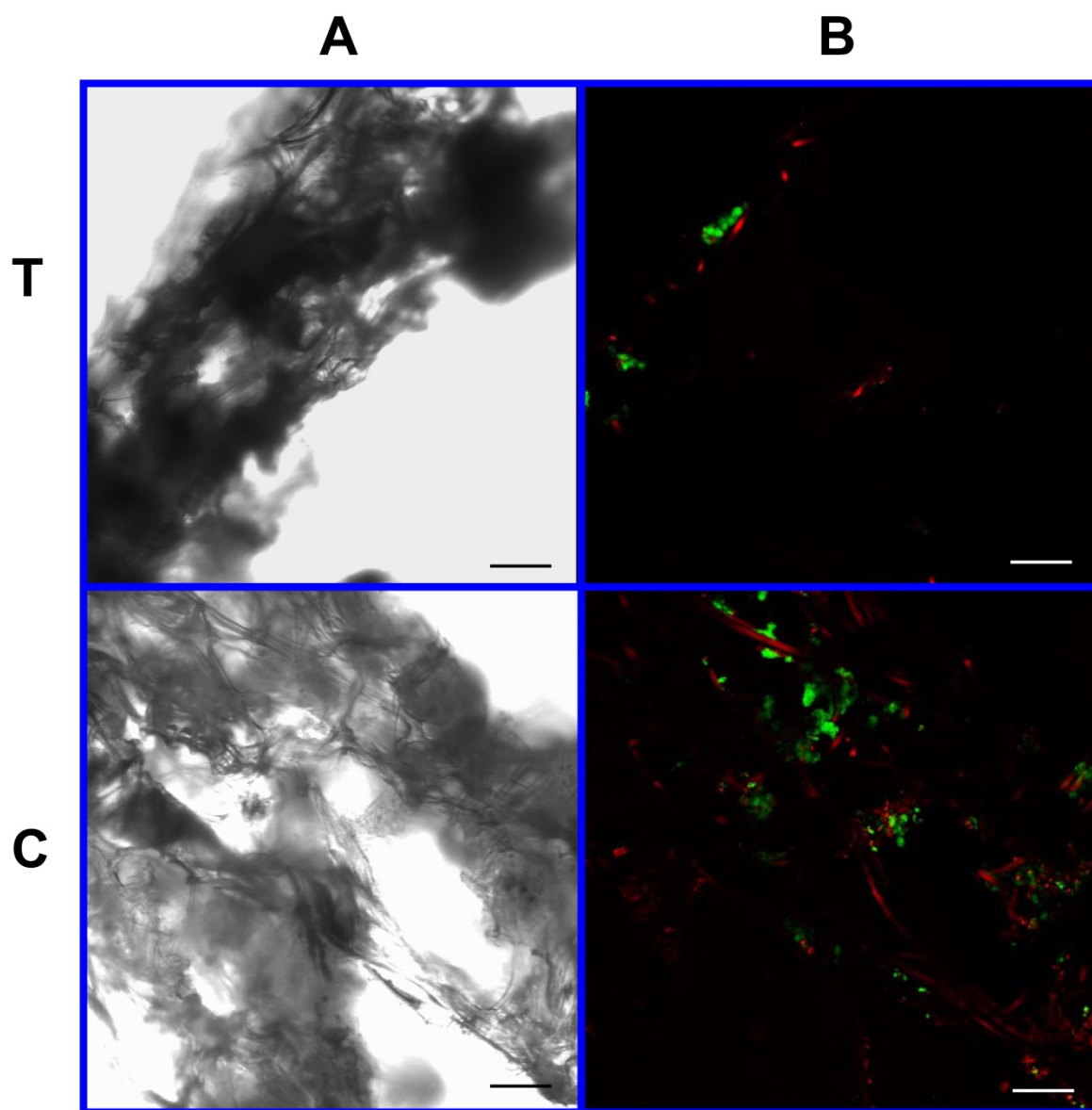
671 100µm.

672

673

674   Figure 12. Photomicrographs of 2% PLLA coated PGA scaffolds harvested on day 10 (row **1**)

675   and day 21 (row **2**), and 4% PLLA coated PGA scaffolds harvested on day 10 (row **3**) and day

676   21 (row **4**), H+E staining. Column **A** represents images of the center of the construct and column

677   **B** represents images taken of the scaffold periphery. Note that the cells have grown in dense

678   clusters; 10x objective magnification; bar = 100µm.

679